

Figure 1. Expression of TIM family members in cultured human mast cell line and primary cells. (a) The mRNA expression for TIM family members (TIM-1, TIM-3 and TIM-4) in a human mast cell line, HMC-1, normal human bronchial epithelial cells (NHBEs) and normal human coronary artery endothelial cells (HCAECs) was determined by quantitative PCR. Human universal reference (HUR) RNA was used as a control. (b) The cell surface expression of TIM family members (TIM-1, TIM-3 and TIM-4) on HMC-1 cells and PBMCs was determined by flow cytometry. Shaded areas=isotype-matched control IgG staining, and bold lines=anti-TIM mAb staining. Data show a representative result of two independent experiments.
 doi:10.1371/journal.pone.0086106.g001

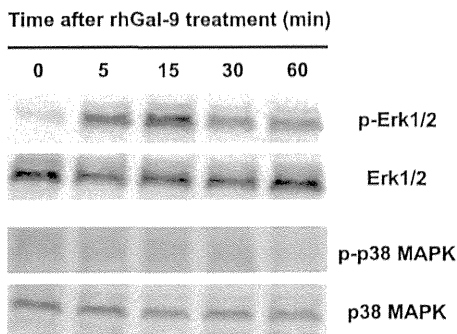


Figure 2. Galectin-9 induces phosphorylation of Erk1/2, but not p38 MAPK, in HMC-1 cells. HMC-1 cells were cultured in the presence of 1 μ M recombinant human galectin-9 (rhGal-9) for the indicated times. Then the levels of phosphorylation of Erk1/2 and p38 MAPK in the cells were determined by western blot analysis. Data show a representative result of three independent experiments. doi:10.1371/journal.pone.0086106.g002

p-nitrophenyl-N-acetyl- β -D-glucosaminide (Sigma Chemical Co.) in 0.1 M sodium citrate (pH 4.5) in a 96-well microtiter plate at 37°C for 1 h. The enzymatic reaction was stopped by addition of 50 μ l of 0.4 M glycine (pH 10.7) to each well. Enzymatic activities (OD405) were measured using a plate reader. Data show the percent release of β -hexosaminidase under various conditions of stimulation relative to the total amount of β -hexosaminidase in the cells, as measured in the supernatants of frozen and thawed cells.

ELISA

HMC-1 cells (1×10^5 cells/well in a 96-well plate) were treated with various concentrations of rhGal-9 in the presence and absence of 20 mM lactose (Nacalai Tesque, Kyoto, Japan) or sucrose (Wako, Osaka, Japan) at 37°C for 18 h. In some cases, HMC-1 cells were treated with ERK inhibitor (PD98059; Calbiochem, La Jolla, CA, USA), ERK inhibitor control (SB202474; Calbiochem) or solvent (0.1% (v/v) DMSO) alone at 37°C for 30 min, and with rhTIM-3-Fc (R&D Systems, Minneapolis, MN, USA) or human IgG (Sigma Chemical Co.) at 37°C for 1 hour before exposure to rhGal-9. The levels of IL-6, IL-8 and MCP-1 in the culture supernatants were determined with ELISA kits (R&D Systems) in accordance with the manufacturer's instructions.

Statistics

All data are expressed as means \pm SD. The unpaired Student's t-test, two-tailed, or ANOVA, as appropriate, was used for statistical evaluation of the results. $P < 0.05$ was considered statistically significant.

Results

Expression of TIM Family Members' mRNA in Human Mast Cell Line

As in our earlier study using mouse mast cells (16), we first examined the expression of mRNA for TIM family members (TIM-1, TIM-3 and TIM-4) in HMC-1 cells and other human primary cells (NHBE and HCAEC, as negative controls) by quantitative PCR. We found constitutive expression of mRNA for both TIM-1 and TIM-3 in HMC-1 cells, but not in NHBE or HCAEC (Figure 1a). On the other hand, expression of TIM-4 mRNA was barely detectable in these cells. Next, we determined the surface protein expression of the TIM family members (TIM-

1, TIM-3 and TIM-4) in HMC-1 cells and PBMCs by flow cytometry. In contrast to mRNA expression, TIM-1 and TIM-3 as well as TIM-4 were barely detectable on either HMC-1 cells or PBMCs (Figure 1b).

Gal-9 Induces Phosphorylation of Erk1/2 in HMC-1 Cells

We previously demonstrated that IL-33 can induce cytokine secretion by human mast cells, although surface expression of ST2, a component of IL-33R, is barely detectable on these cells by flow cytometry [33]. Likewise, although surface expression of TIM-3 is barely detectable on HMC-1 cells, Gal-9, which is a ligand for TIM-3, may play some role in activation and/or regulation of HMC-1 cells. Thus, we examined the effect of rhGal-9 on the phosphorylation of signaling molecules in those cells by immunoblot analysis. We found that rhGal-9 induced phosphorylation of Erk1/2, but not p38 MAPK, in HMC-1 cells (Figure 2), suggesting that rhGal-9 may influence the function of HMC-1 cells.

Gal-9 Induces Apoptosis of HMC-1 Cells

We next examined the effects of Gal-9 on HMC-1 cell survival. After treatment with or without mitomycin C, HMC-1 cells were cultured in the presence and absence of 0.25, 0.5 and 1 μ M rhGal-9 for 24, 48 and 72 hours. The number of trypan blue-negative viable cells was significantly decreased by 1 μ M rhGal-9, while the percentage of propidium iodide-negative and annexin V-positive apoptotic cells was significantly increased irrespective of mitomycin C treatment (Figure 3a and 3b). In association with this, as in the case of staurosporine treatment, the levels of caspase-3/7 activity in HMC-1 cells were also significantly increased after rhGal-9 treatment (Figure 3c). These findings indicate that rhGal-9 induces apoptosis of HMC-1 cells.

Gal-9 Inhibits Degranulation of HMC-1 Cells

We next evaluated the effect of rhGal-9 on degranulation of HMC-1 cells. HMC-1 cells were treated with 0, 0.25, 0.5 and 1 μ M of rhGal-9 for 30 min prior to stimulation with PMA+ionomycin. The level of degranulation, assessed by the release of β -hexosaminidase from the cells, was significantly suppressed by pretreatment with the optimal dose (0.5 μ M) of rhGal-9 (Figure 4a). In the setting, pre-treatment with 0.5 μ M rhGal-9 resulted in inhibition of cell survival (assessed as trypan blue-negative cells, and propidium iodide-negative and annexin V-positive apoptotic cells by flow cytometry) as well as degranulation after stimulation with PMA+ionomycin (Figure 4b–d), suggesting that the reduced degranulation of HMC-1 cells may be due to apoptosis of the cells after rhGal-9 treatment. On the other hand, the relative levels of degranulation per live HMC-1 cells were significantly reduced by pre-treatment with rhGal-9 (Figure 4e), suggesting that Gal-9 also inhibited PMA- and ionomycin-induced degranulation of HMC-1 cells independently of Gal-9-mediated apoptosis. Thus, these observations suggest that Gal-9 can inhibit PMA- and ionomycin-induced degranulation of HMC-1 cells, both directly and indirectly.

Gal-9 Induces Cytokine Production by HMC-1 Cells

In contrast to the inhibitory effect of rhGal-9 on degranulation, we found that IL-6, IL-8 and MCP-1 production by HMC-1 cells was dose-dependently induced by rhGal-9 (Figure 5a). It is known that most biological effects of galectins are mediated by their carbohydrate-binding activities. [5] In support of that, rhGal-9-mediated IL-6 production by HMC-1 cells was strongly suppressed by addition of an excessive amount of lactose but not sucrose (Figure 5b). Moreover, rhGal-9-mediated IL-6 production

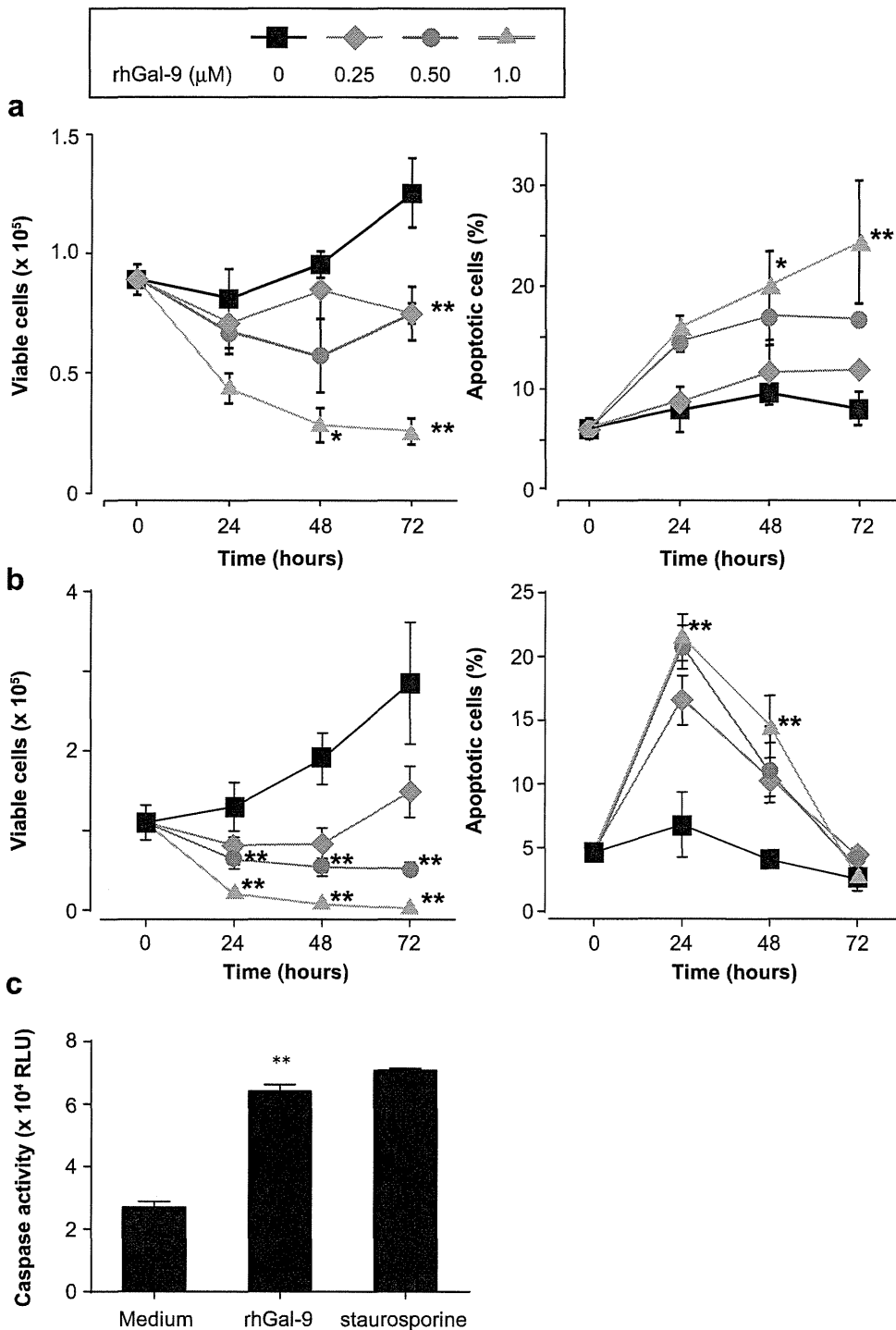


Figure 3. Galectin-9 induces apoptosis of HMC-1 cells. (a, b) HMC-1 cells pre-treated with (a) or without mitomycin C (b) were cultured in the presence of 0, 0.25, 0.5 or 1 μ M recombinant human galectin-9 (rhGal-9) for the indicated time periods. The number of viable cells was determined by trypan blue staining. The proportion of propidium iodide-negative and annexin V-positive apoptotic cells was assessed by flow cytometry. (c) HMC-1 cells (no mitomycin C pre-treatment) were cultured in the presence and absence of 0.5 μ M rhGal-9 or 0.1 μ M staurosporine for 16 hours. Then the levels of caspase activity in the cells were determined. Data show the mean \pm SD of triplicate samples and are a representative result of three independent experiments. * p <0.05 and ** p <0.01 versus the corresponding values for the vehicle control. doi:10.1371/journal.pone.0086106.g003

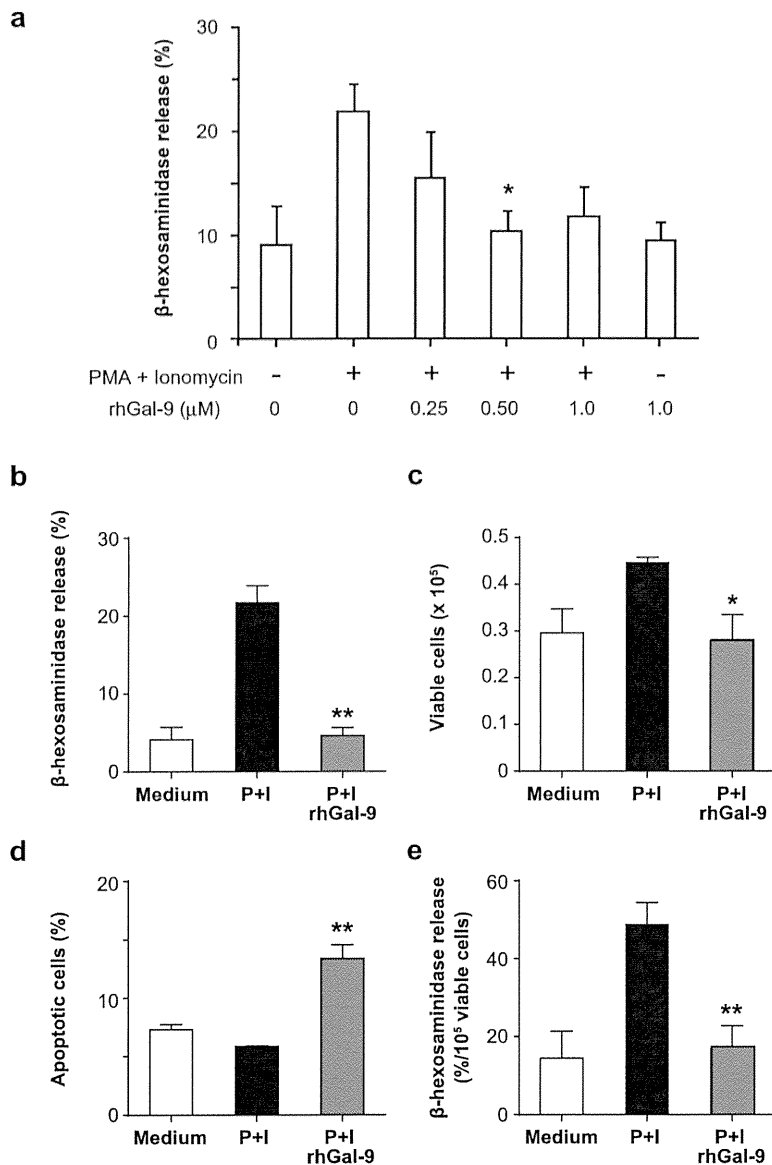


Figure 4. Galectin-9 inhibits PMA- and ionomycin-dependent degranulation of HMC-1 cells. (a, b) HMC-1 cells were treated with 0, 0.25, 0.5 or 1 μM (a) and 0 or 0.5 μM (b) recombinant human galectin-9 (rhGal-9) for 30 min. The cells were then stimulated with 0.1 μg/ml PMA +1 μg/ml ionomycin for 30 min. The level of degranulation was assessed from the activity of β-hexosaminidase in the culture supernatant and plotted as the percent release. (c) The number of viable cells in (b) was determined by trypan blue staining. (d) The proportion of propidium iodide-negative and annexin V-positive apoptotic cells in (b) was assessed by flow cytometry. (e) The relative level of degranulation per live HMC-1 cells was determined as (b)/(c). Data show the mean ± SD of triplicate samples and are a representative result of three (a) or two (b–e) independent experiments. * $p < 0.05$, ** $p < 0.01$ versus PMA+ionomycin alone. doi:10.1371/journal.pone.0086106.g004

by HMC-1 cells was inhibited by addition of a soluble form of TIM-3 (rhTIM-3/Fc) but not control human IgG (Figure 5c), and by pre-treatment with PD98059 (an ERK1/2 inhibitor) but not SB202474 (control for the ERK1/2 inhibitor) (Figure 5d), suggesting that Gal-9-mediated ERK1/2 activation is required for cytokine production by HMC-1 cells.

Discussion

In the present study, we demonstrated that Gal-9 has dual roles in the functions of a human mast cell line, HMC-1. That is, Gal-9

reduced survival by inducing apoptosis and suppressed degranulation in HMC-1 cells, while it induced cytokine and chemokine production by these cells by activating ERK1/2.

We show that Gal-9 induced phosphorylation of Erk1/2, but not p38 MAPK, in HMC-1 cells (Figure 2). On the other hand, however, Gal-9 induced maturation of human monocyte-derived DCs through activation of p38 MAPK, but not ERK1/2. [34] These observations suggest that the Gal-9-mediated signaling pathway may be different in distinct types of cells. Alternatively, the difference between DCs and HMC-1 cells may be mediated by

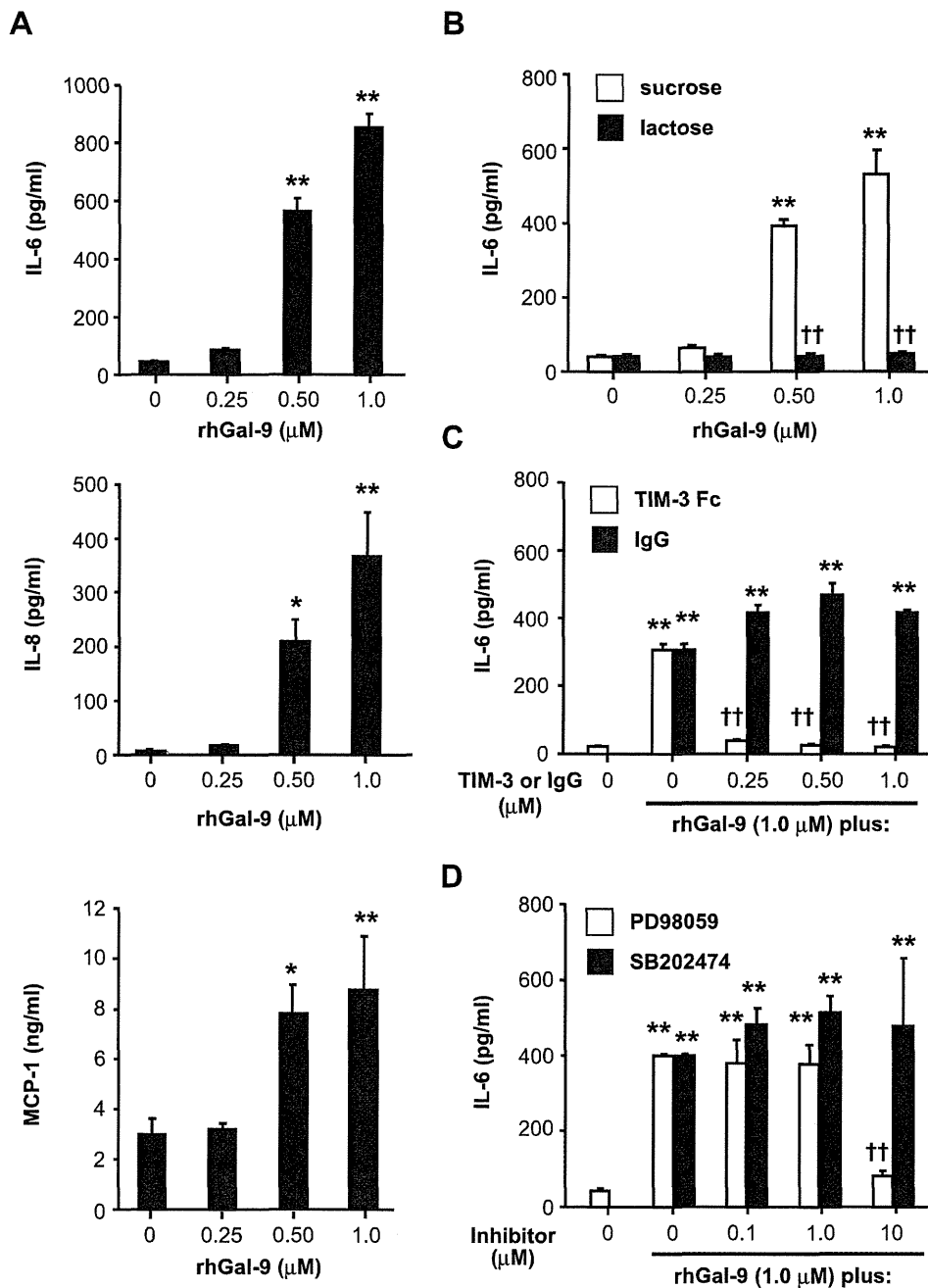


Figure 5. Gal-9 induces cytokine and chemokine production by HMC-1 cells. ELISA was performed to determine the levels of IL-6, IL-8 and MCP-1 in the culture supernatants of HMC-1 cells (a), HMC-1 cells pre-treated with 20 mM lactose or sucrose (b), HMC-1 cells pre-treated with recombinant human TIM-3/Fc (rhTIM-3/Fc) or control human IgG (human IgG) (c) and HMC-1 cells pre-treated with ERK inhibitor (PD98059) or its control (SB202474) (d) after 18 hours' stimulation with 0, 0.25, 0.5 or 1 μM recombinant human Galectin-9 (rhGal-9). Data show the mean \pm SD of triplicate samples and are a representative result of three independent experiments. * $p < 0.05$ and/or ** $p < 0.01$ versus 0 μM rhGal-9 (a-d), and † $p < 0.05$ and/or †† $p < 0.01$ versus sucrose (b), control human IgG (c) or ERK inhibitor control (d). doi:10.1371/journal.pone.0086106.g005

distinct receptors such as TIM-3 and unknown molecules that interact with Gal-9. Indeed, the lectin property of Gal-9 was required for Gal-9-mediated cytokine production by HMC-1 cells (Figure 5b), but not by human DCs. [34] In addition, Gal-9 induced apoptosis of HMC-1 cells (Figure 3) as well as thymocytes,

Th1 cells and Th17 cells in mice, and human melanoma cell lines. [2,7,21–23,35] In contrast, we previously demonstrated that anti-TIM-3 antibody, which enhanced IgE/Ag-mediated cytokine production as an agonistic antibody, suppressed apoptosis of IL-3-induced mouse bone marrow cell-derived cultured mast cells. [16]

These observations suggest that Gal-9-mediated responses may be dependent or independent of TIM-3, in different cells, since TIM-3 is also known to bind to phosphatidylserine. [36].

It was shown that Gal-9 bound IgE, resulting in inhibition of IgE/antigen-FcεRI-mediated degranulation in mouse mast cell lines by preventing IgE/antigen complex formation. [29] In the present study, because HMC-1 cells do not express FcεRI, [37] we assessed the effect of Gal-9 on PMA/ionomycin-mediated degranulation of HMC-1 cells. Figure 4 shows that Gal-9 suppressed that degranulation both directly and indirectly, suggesting that there might be distinct mechanisms underlying the inhibitory effects of Gal-9 on IgE/antigen-FcεRI-mediated and PMA/ionomycin-mediated mast cell degranulation.

Studies in rodents found that treatment with Gal-9 before antigen challenge resulted in attenuation of ovalbumin- and mite allergen-induced allergic airway inflammation as well as passive cutaneous anaphylaxis after antigen challenge. [27,29] Gal-9's attenuation of such disorders in mast cells [29] was due to suppression of degranulation, rather than induction of cytokines and chemokines, probably independent of TIM-3, since TIM-3-deficient mice normally developed allergic airway inflammation. [28] However, treatment with Gal-9 after antigen challenge may

exacerbate inflammation in the late phase of allergic diseases by enhancing cytokine and chemokine production by mast cells and recruiting eosinophils to local inflammatory sites.

In conclusion, Gal-9 appears to play dual roles in the function of human mast cell line. Our results suggest that Gal-9 may modulate the induction and progression of allergic diseases by suppressing degranulation and enhancing cytokine and chemokine production of mast cells. In addition, Gal-9 may be a potential therapeutic target for immediate allergic reactions induced by mast cell degranulation.

Acknowledgments

We are grateful to Lawrence W. Stiver (Tokyo, Japan) for critical reading of the manuscript.

Author Contributions

Conceived and designed the experiments: TO MI S. Nakae. Performed the experiments: RK TO. Analyzed the data: RK TO S. Nakae. Contributed reagents/materials/analysis tools: MI TN MH KI HT S. Nonoyama AM HS KM. Wrote the paper: RK TO S. Nakae.

References

- Matsumoto R, Hirashima M, Kita H, Gleich GJ (2002) Biological activities of ecalectin: a novel eosinophil-activating factor. *J Immunol* 168: 1961–1967.
- Matsumoto R, Matsumoto H, Seki M, Hata M, Asano Y, et al. (1998) Human ecalectin, a variant of human galectin-9, is a novel eosinophil chemoattractant produced by T lymphocytes. *J Biol Chem* 273: 16976–16984.
- Matsushita N, Nishi N, Seki M, Matsumoto R, Kuwabara I, et al. (2000) Requirement of divalent galactoside-binding activity of ecalectin/galectin-9 for eosinophil chemoattraction. *J Biol Chem* 275: 8355–8360.
- Asakura H, Kashio Y, Nakamura K, Seki M, Dai S, et al. (2002) Selective eosinophil adhesion to fibroblast via IFN- γ -induced galectin-9. *J Immunol* 169: 5912–5918.
- Hirashima M, Kashio Y, Nishi N, Yamauchi A, Imaizumi TA, et al. (2004) Galectin-9 in physiological and pathological conditions. *Glycoconj J* 19: 593–600.
- Seki M, Sakata KM, Oomizu S, Arikawa T, Sakata A, et al. (2007) Beneficial effect of galectin 9 on rheumatoid arthritis by induction of apoptosis of synovial fibroblasts. *Arthritis Rheum* 56: 3968–3976.
- Wada J, Ota K, Kumar A, Wallner EI, Kanwar YS (1997) Developmental regulation, expression, and apoptotic potential of galectin-9, a beta-galactoside binding lectin. *J Clin Invest* 99: 2452–2461.
- Rabinovich GA, Liu FT, Hirashima M, Anderson A (2007) An emerging role for galectins in tuning the immune response: lessons from experimental models of inflammatory disease, autoimmunity and cancer. *Scand J Immunol* 66: 143–158.
- Zhu C, Anderson AC, Schubart A, Xiong H, Imitola J, et al. (2005) The Tim-3 ligand galectin-9 negatively regulates T helper type 1 immunity. *Nat Immunol* 6: 1245–1252.
- Monney L, Sabatos CA, Gaglia JL, Ryu A, Waldner H, et al. (2002) Th1-specific cell surface protein Tim-3 regulates macrophage activation and severity of an autoimmune disease. *Nature* 415: 536–541.
- Nakae S, Iwakura Y, Suto H, Galli SJ (2007) Phenotypic differences between Th1 and Th17 cells and negative regulation of Th1 cell differentiation by IL-17. *J Leukoc Biol* 81: 1258–1268.
- Ndhlovu LC, Lopez-Verges S, Barbour JD, Jones RB, Jha AR, et al. (2012) Tim-3 marks human natural killer cell maturation and suppresses cell-mediated cytotoxicity. *Blood* 119: 3734–3743.
- Liu Y, Shu Q, Gao L, Hou N, Zhao D, et al. (2010) Increased Tim-3 expression on peripheral lymphocytes from patients with rheumatoid arthritis negatively correlates with disease activity. *Clin Immunol* 137: 288–295.
- Tang ZH, Liang S, Potter J, Jiang X, Mao HQ, et al. (2013) Tim-3/galectin-9 regulate the homeostasis of hepatic NKT cells in a murine model of nonalcoholic fatty liver disease. *J Immunol* 190: 1788–1796.
- Anderson AC, Anderson DE, Bregoli L, Hastings WD, Kassam N, et al. (2007) Promotion of tissue inflammation by the immune receptor Tim-3 expressed on innate immune cells. *Science* 318: 1141–1143.
- Nakae S, Iikura M, Suto H, Akiba H, Umetsu DT, et al. (2007) TIM-1 and TIM-3 enhancement of Th2 cytokine production by mast cells. *Blood* 110: 2565–2568.
- Wiener Z, Kohalmi B, Pocza P, Jeager J, Tolgyesi G, et al. (2007) TIM-3 is expressed in melanoma cells and is upregulated in TGF- β stimulated mast cells. *J Invest Dermatol* 127: 906–914.
- Nobumoto A, Oomizu S, Arikawa T, Katoh S, Nagahara K, et al. (2009) Galectin-9 expands unique macrophages exhibiting plasmacytoid dendritic cell-like phenotypes that activate NK cells in tumor-bearing mice. *Clin Immunol* 130: 322–330.
- Nagahara K, Arikawa T, Oomizu S, Kontani K, Nobumoto A, et al. (2008) Galectin-9 increases Tim-3+ dendritic cells and CD8+ T cells and enhances antitumor immunity via galectin-9-Tim-3 interactions. *J Immunol* 181: 7660–7669.
- Irie A, Yamauchi A, Kontani K, Kihara M, Liu D, et al. (2005) Galectin-9 as a prognostic factor with antimetastatic potential in breast cancer. *Clin Cancer Res* 11: 2962–2968.
- Kageshita T, Kashio Y, Yamauchi A, Seki M, Abedin MJ, et al. (2002) Possible role of galectin-9 in cell aggregation and apoptosis of human melanoma cell lines and its clinical significance. *Int J Cancer* 99: 809–816.
- Wiersma VR, de Bruyn M, van Ginkel RJ, Sigar E, Hirashima M, et al. (2012) The glycan-binding protein galectin-9 has direct apoptotic activity toward melanoma cells. *J Invest Dermatol* 132: 2302–2305.
- Seki M, Oomizu S, Sakata KM, Sakata A, Arikawa T, et al. (2008) Galectin-9 suppresses the generation of Th17, promotes the induction of regulatory T cells, and regulates experimental autoimmune arthritis. *Clin Immunol* 127: 78–88.
- Kearley J, McMillan SJ, Lloyd GM (2007) Th2-driven, allergen-induced airway inflammation is reduced after treatment with anti-Tim-3 antibody in vivo. *J Exp Med* 204: 1289–1294.
- Sziksz E, Kozma GT, Pallinger E, Komlosi ZI, Adori C, et al. (2010) Galectin-9 in allergic airway inflammation and hyper-responsiveness in mice. *Int Arch Allergy Immunol* 151: 308–317.
- Yamamoto H, Kashio Y, Shoji H, Shinonaga R, Yoshimura T, et al. (2007) Involvement of galectin-9 in guinea pig allergic airway inflammation. *Int Arch Allergy Immunol* 143 Suppl 1: 95–105.
- Katoh S, Ishii N, Nobumoto A, Takeshita K, Dai SY, et al. (2007) Galectin-9 inhibits CD44-hyaluronan interaction and suppresses a murine model of allergic asthma. *Am J Respir Crit Care Med* 176: 27–35.
- Barlow JL, Wong SH, Ballantyne SJ, Jolin HE, McKenzie AN (2011) Tim1 and Tim3 are not essential for experimental allergic asthma. *Clin Exp Allergy* 41: 1012–1021.
- Niki T, Tsutsui S, Hirose S, Aradono S, Sugimoto Y, et al. (2009) Galectin-9 is a high affinity IgE-binding lectin with anti-allergic effect by blocking IgE-antigen complex formation. *J Biol Chem* 284: 32344–32352.
- Butterfield JH, Weiler D, Dewald G, Gleich GJ (1988) Establishment of an immature mast cell line from a patient with mast cell leukemia. *Leuk Res* 12: 345–355.
- Yagami A, Orihara K, Morita H, Futamura K, Hashimoto N, et al. (2010) IL-33 mediates inflammatory responses in human lung tissue cells. *J Immunol* 185: 5743–5750.
- Ho LH, Ohno T, Oboki K, Kajiwara N, Suto H, et al. (2007) IL-33 induces IL-13 production by mouse mast cells independently of IgE-Fcεp150R1 signals. *J Leukoc Biol* 82: 1481–1490.
- Iikura M, Suto H, Kajiwara N, Oboki K, Ohno T, et al. (2007) IL-33 can promote survival, adhesion and cytokine production in human mast cells. *Lab Invest* 87: 971–978.

34. Dai SY, Nakagawa R, Itoh A, Murakami H, Kashio Y, et al. (2005) Galectin-9 induces maturation of human monocyte-derived dendritic cells. *J Immunol* 175: 2974–2981.
35. Kashio Y, Nakamura K, Abedin MJ, Seki M, Nishi N, et al. (2003) Galectin-9 induces apoptosis through the calcium-calpain-caspase-1 pathway. *J Immunol* 170: 3631–3636.
36. Nakayama M, Akiba H, Takeda K, Kojima Y, Hashiguchi M, et al. (2009) Tim-3 mediates phagocytosis of apoptotic cells and cross-presentation. *Blood* 113: 3821–3830.
37. Xia HZ, Kopley CL, Sakai K, Chelliah J, Irani AM, et al. (1995) Quantitation of tryptase, chymase, Fc epsilon RI alpha, and Fc epsilon RI gamma mRNAs in human mast cells and basophils by competitive reverse transcription-polymerase chain reaction. *J Immunol* 154: 5472–5480.

ORIGINAL ARTICLE

Mutations of *NOTCH3* in childhood pulmonary arterial hypertension

Ayako Chida^{1,2}, Masaki Shintani², Yoshihisa Matsushita², Hiroki Sato³, Takahiro Eitoku⁴, Tomotaka Nakayama⁵, Yoshiyuki Furutani², Emiko Hayama², Yoichi Kawamura¹, Kei Inai², Shinichi Ohtsuki⁴, Tsutomu Saji⁵, Shigeaki Nonoyama¹ & Toshio Nakanishi²

¹Department of Pediatrics, National Defense Medical College, 3-2 Namiki, Tokorozawa, Saitama, 359-8513, Japan

²Department of Pediatric Cardiology, Tokyo Women's Medical University, 8-1 Kawada-cho, Shinjuku-ku, Tokyo, 162-8666, Japan

³Department of Preventive Medicine and Public Health, National Defense Medical College, 3-2 Namiki, Tokorozawa, Saitama, 359-8513, Japan

⁴Division of Pediatric Cardiology, Department of Pediatrics, Okayama University, 2-5-1 Shikata-cho, Okayama, 700-8558, Japan

⁵Department of Pediatrics, Toho University Medical Center, Omori Hospital, 6-11-1 Omori-nishi, Ota-ku, Tokyo, Japan

Keywords

ER stress, gene mutation, *NOTCH3*, pulmonary arterial hypertension

Correspondence

Toshio Nakanishi, Department of Pediatric Cardiology, Tokyo Women's Medical University, 8-1 Kawada-cho, Shinjuku-ku, Tokyo, 162-8666, Japan. Tel: +81-3-3353-8112; Fax: +81-3-3352-3088; E-mail: pnakanis@hij.tvmu.ac.jp

Funding Information

This work was supported by MEXT KAKENHI grant number 24591588.

Received: 13 August 2013; Revised: 2 November 2013; Accepted: 12 November 2013

doi: 10.1002/mgg3.58

Abstract

Mutations of *BMPR2* and other TGF- β superfamily genes have been reported in pulmonary arterial hypertension (PAH). However, 60–90% of idiopathic PAH cases have no mutations in these genes. Recently, the expression of *NOTCH3* was shown to be increased in the pulmonary artery smooth muscle cells of PAH patients. We sought to investigate *NOTCH3* and its target genes in PAH patients and clarify the role of *NOTCH3* signaling. We screened for mutations in *NOTCH3*, *HES1*, and *HES5* in 41 PAH patients who had no mutations in *BMPR2*, *ALK1*, *endoglin*, *SMAD1/4/8*, *BMPR1B*, or *Caveolin-1*. Two novel missense mutations (c.2519 G>A p.G840E, c.2698 A>C p.T900P) in *NOTCH3* were identified in two PAH patients. We performed functional analysis using stable cell lines expressing either wild-type or mutant *NOTCH3*. The protein-folding chaperone GRP78/BiP was colocalized with wild-type *NOTCH3* in the endoplasmic reticulum, whereas the majority of GRP78/BiP was translocated into the nuclei of cells expressing mutant *NOTCH3*. Cell proliferation and viability were higher for cells expressing mutant *NOTCH3* than for those expressing wild-type *NOTCH3*. We identified novel *NOTCH3* mutations in PAH patients and revealed that these mutations were involved in cell proliferation and viability. *NOTCH3* mutants induced an impairment in *NOTCH3*-*HES5* signaling. The results may contribute to the elucidation of PAH pathogenesis.

Introduction

Pulmonary arterial hypertension (PAH) is a progressive, severe, potentially fatal disease with an estimated incidence of approximately 1–2 patients per million per year (Gaine and Rubin 1998). Idiopathic PAH (IPAH) is a sporadic form of the disease in which there is neither a family history of PAH nor an identified risk factor (Simonneau et al. 2009). Heritable PAH (HPAH) is inherited in an autosomal dominant fashion with 10–20% penetrance, and affects females approximately twice as often as males (Machado et al. 2009).

Bone morphogenetic protein (BMP) receptor 2 (*BMPR2*), a member of the transforming growth factor

(TGF)- β superfamily, was identified as a primary gene for HPAH in 2000 (Deng et al. 2000; Lane et al. 2000). Subsequent studies of the TGF- β superfamily revealed additional genes responsible for PAH: activin receptor-like kinase 1 (*ALK1*), *endoglin* (*ENG*), *SMAD1/4/8*, and bone morphogenetic protein receptor 1B (*BMPR1B*) (Trembath et al. 2001; Harrison et al. 2003, 2005; Shintani et al. 2009; Chida et al. 2012; Nasim et al. 2012). In addition, Austin et al. (2012) identified *Caveolin-1* (*CAV1*) mutations in PAH patients using whole exome sequencing. These genetic studies have considerably enhanced our understanding of the molecular basis of PAH. However, almost 30% of HPAH cases and 60–90% of IPAH cases have no mutations in *BMPR2*, *ALK1*, *ENG*, *SMAD 1/4/8*, *BMPR1B*, or *CAV1*.

In 2009, Li et al. reported that human pulmonary hypertension could be characterized by the overexpression of *NOTCH3* (OMIM 600276) in small pulmonary artery smooth muscle cells (SMCs), and that the severity of the disease in humans and rodents is correlated with the amount of *NOTCH3* protein in the lungs (Li et al. 2009). Therefore, we hypothesized that genes belonging to the *NOTCH3* signaling pathways, in addition to the BMP signaling pathway, may be associated with the onset of IPAH/HPAH. Accordingly, we screened for mutations in *NOTCH3* and its target genes, *HES1* and *HES5*.

Materials and Methods

Subjects

From a previous screen of patients with IPAH/HPAH (Shintani et al. 2009; Chida et al. 2012), we identified 41 patients who did not have mutation in *BMPR2*, *ALK1*, *SMAD1*, *SMAD4*, *SMAD8*, *BMPR1B*, or *CAV1*. These patients formed the basis of this study (Fig. 1). The diagnosis of IPAH/HPAH was made through a clinical evaluation, echocardiography, and cardiac catheterization based on the following criteria: mean pulmonary artery pressure >25 mmHg at rest (Galiè et al. 2009). Patients with PAH associated with another disease, such as portal hypertension or congenital heart disease, were excluded from this study by trained cardiologists. This study was approved by the Institutional Review Committee of Tokyo Women's Medical University. Written informed consent

was obtained from all patients or their guardians in accordance with the Declaration of Helsinki.

Molecular analysis

For the 41 patients with no mutations in *BMPR2*, *ALK1*, *SMAD 1/4/8*, *BMPR1B*, or *CAV1*, all coding exons and adjacent intronic regions for *NOTCH3*, *HES1*, and *HES5* were amplified from the genomic DNA using polymerase chain reactions (PCR primer details are available in Table S1). PCR-amplified products were purified and screened via bidirectional direct sequencing with an ABI 3130xl DNA Analyzer (Applied Biosystems, CA). All of the generated sequences were compared with wild-type *NOTCH3* (GenBank NM_000435), *HES1* (GenBank NM_005524), and *HES5* (GenBank NM_001010926).

Stable cell lines

We established stable HEK293 cell lines in which the expression of *NOTCH3* was inducible using the tetracycline regulatory system because it was known that the expression of *NOTCH3* in vascular SMCs caused excessive cell death as early as 2 days after transfection (Takahashi et al. 2010). T-REx 293 cells (Invitrogen, Carlsbad, CA) were grown in high glucose DMEM (Sigma, St Louis, MO) supplemented with 10% fetal bovine serum (Gibco, Grand Island, NY), 2 mmol/L L-glutamine, and 5 µg/mL blasticidin (Gibco). The wild-type and mutant *NOTCH3* constructs were transfected into T-REx 293 cells using Lipofectamine 2000 reagent (Invitrogen). After 48 h, cells were selected in the presence of 100 µg/mL Zeocin and 5 µg/mL Blasticidin-S (Invitrogen). After treatment with tetracycline (Tet; 2 µg/mL) for 24 h, the expression level of *NOTCH3* was determined by western blotting using AbN2. Stable cell lines were maintained in high glucose DMEM-containing 10% fetal bovine serum, 5 µg/mL Zeocin, and 5 µg/mL Blasticidin-S.

Preparation of plasmids, antibodies, and ligands

Human pcDNA4/TO-*NOTCH3* was kindly provided by Dr. Atsushi Watanabe (Aichi, Japan). The reporter gene construct pHes5-luc was a kind gift from Dr. Ryoichiro Kageyama (Kyoto, Japan). Site-directed mutagenesis was carried out using a site-directed mutagenesis kit (Stratagene, CA). The antibodies used were as follows: rabbit polyclonal anti-human *NOTCH3* antibodies (AbN2; gifts from A. Watanabe), monoclonal *NOTCH3* antibody (3A2; gift from A. Watanabe), anti-β actin mouse antibody (Sigma-Aldrich, MO), anti-mouse ERp72 antibody, anti-mouse Calnexin antibody, and anti-mouse BiP/GRP78 antibody (R&D Systems, Oxon, UK). AbN2 and 3A2 have

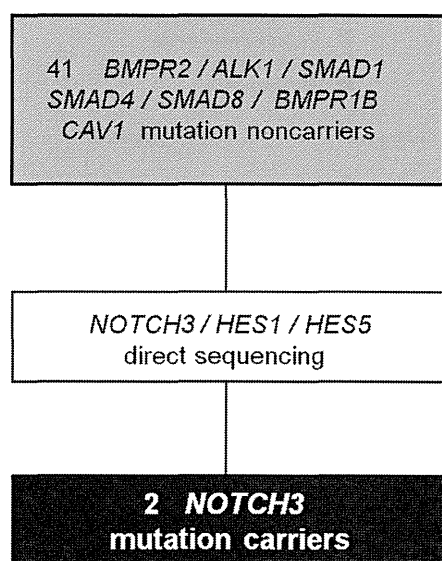


Figure 1. Patient disposition.

previously been shown to specifically recognize the *NOTCH3* protein (Takahashi et al. 2010). Recombinant human Jagged-1 Fc chimera and human BMP4 enzyme-linked immunosorbent assays were from R&D Systems.

Statistical analysis

Data are presented as means with standard deviation (SD). Differences between the means were evaluated by the Dunnett’s test following one-way or two-way analysis of variance (ANOVA). Values of $P < 0.05$ were considered significant. All statistical analyses were performed using SAS version 9.3 (SAS Institute, Cary, NC).

The methods of western blotting and immunoprecipitation, immunocytochemistry, luciferase assay, and cell proliferation and viability tests are detailed in the Data S1.

Results

Identification of two novel *NOTCH3* mutations

We screened for mutations in the *NOTCH3*, *HES1*, and *HES5* genes in 41 IPAH/HPAH patients who had no

mutations in *BMPR2*, *ALK1*, *ENG*, *SMAD1/4/8*, *BMPR1B*, or *CAVI* (Fig. 1). In these 41 patients, the median age at diagnosis was 9 years (range: 0–62 years). The number of male patients was 18 (44 %). Although no mutations were identified in *HES1* or *HES5*, we identified two *NOTCH3* missense mutations in two independent probands with IPAH: a c.2519 G>A p.G840E mutation in proband A, and a c.2698 A>C p.T900P mutation in proband B (Fig. 2A). As depicted in Figure 2B, *NOTCH3* consists of 34 epidermal growth factor (EGF)-like repeats, three Notch/Lin-12 repeats, a transmembrane domain, seven ankyrin repeats, and a PEST sequence (rich in proline [P], glutamic acid [E], serine [S], and threonine [T]). Both the G840E and T900P mutations were located in the EGF-like repeats. The alignment of the *NOTCH3* protein of nine distantly related species showed that the G840 and T900 amino acids were highly conserved (Fig. 2C). The G840E and T900P mutations were absent in 170 Japanese healthy controls and additional 300 Caucasian healthy controls and were not found in the 1000 Genomes Database (<http://www.1000genomes.org>) or the Exome Variant Server (EVS) Database (evs.gs.washington.edu/EVS). Besides, in Polyphen-2 (Polymorphism phenotyping v2) (Adzhubei et al. 2010) and the SIFT

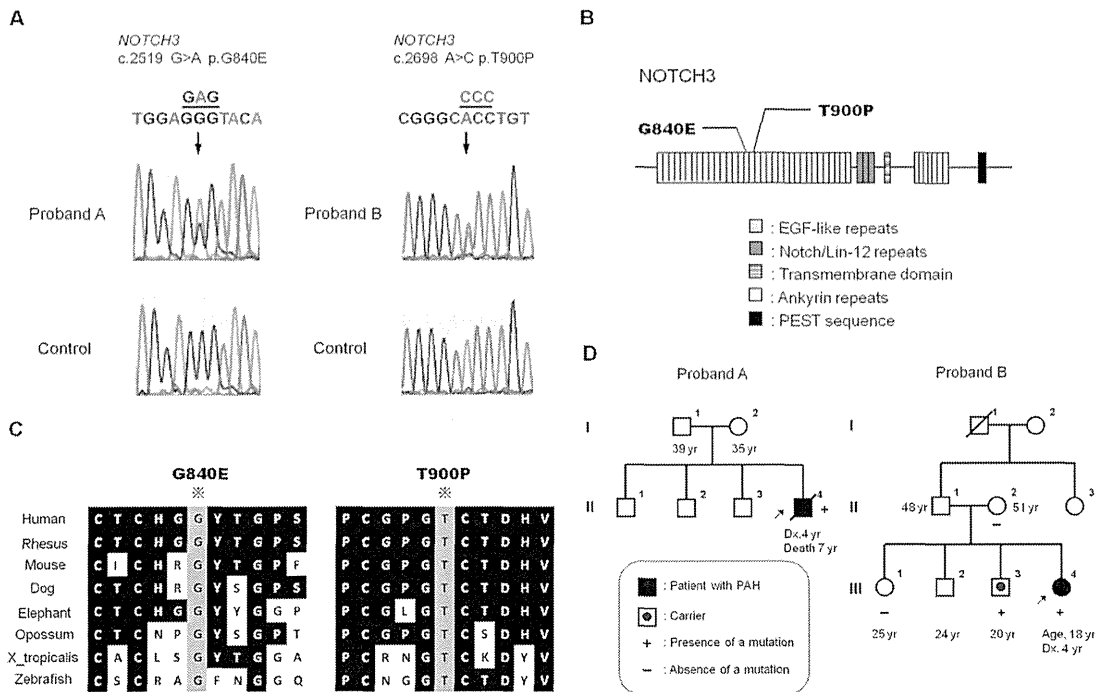


Figure 2. *NOTCH3* mutations in idiopathic pulmonary arterial hypertension patients. (A) Two mutations, c.2519 G>A p.G840E and c.2698 A>C p.T900P, were identified in two probands. (B) Schematic representation of the wild-type *NOTCH3* protein and the locations of the two mutations. (C) Alignment of *NOTCH3* proteins among human, rhesus monkey, mouse, dog, elephant, opossum, chicken, *Xenopus tropicalis*, and zebrafish, showing the conservation of glycine 840 and threonine 900 in these species. (D) Pedigrees of the patients’ families. The current age or the age at diagnosis (Dx) is provided for each family member.

Human Protein (Kumar et al. 2009), both variants were regarded as “Probably damaging” and “Damaging,” respectively.

In proband A, there was no family history of PAH (Fig. 2D). The subject’s family members were not screened for *NOTCH3* mutations because their blood samples could not be obtained. Although there was no family history of PAH in proband B, the same mutation was identified in the patient’s youngest elder brother (Figs. 2D and S1). The patient’s mother and elder sister did not have the mutation. The other family members of proband B were not screened for *NOTCH3* mutations because their blood samples could not be obtained.

Clinical characteristics of patients

Proband A

When the patient was 4 years old, he visited the clinic because of upper respiratory inflammation. A physical examination revealed a cardiac murmur. Cardiomegaly was identified by a chest X-ray and the patient was diagnosed with IPAH. The hemodynamic data of the patient at 5 years of age revealed a mean pulmonary arterial pressure (mPAP) of 70 mmHg and a right atrial pressure (RAP) of 7 mmHg. The patient’s condition progressed to the World Health Organization (WHO) functional class II at 5 years of age. The patient had been administered sildenafil, bosentan, beraprost, and warfarin since the age of 4. When he was 5 years old, the patient began home oxygen therapy (HOT) and diuretics. He did not receive epoprostenol because his family’s consent was not obtained. The patient’s condition deteriorated despite increases in the doses of sildenafil, bosentan, and veraprost. The patient suffered cardiopulmonary arrest caused by pulmonary hypertension crisis at 6 years old; he was successfully resuscitated and began intravenous epoprostenol therapy. Although the dose of epoprostenol was increased gradually, the patient’s heart failure worsened. When he was 7 years old, the patient was discharged from hospital after beginning home intravenous epoprostenol. However, the patient died 9 days later because of a pulmonary hemorrhage.

The patient’s past history included brain infarction and right hemiparesis caused by Moyamoya disease. The patient had left cerebral arterial revascularization surgery when he was 3 years old. No complications were reported in the aorta or renal arteries.

Proband B

This patient’s first symptom was fatigue at 4 years of age. At the initial visit, the patient’s right ventricle

pressure was almost equal to left ventricle pressure and her brain natriuretic peptide level was 1380 pg/mL. Although the patient was administered beraprost, she became more impaired, and began intravenous epoprostenol at the age of 5. This therapy was initially very effective; however, the patient’s mPAP progressively increased. Increasing the amount of epoprostenol and administering sildenafil and bosentan were not effective. The patient’s hemodynamic data at 15 years of age revealed an mPAP of 67 mmHg, a RAP of 12 mmHg, a CI of 2.9 L min⁻¹ m⁻², and a pulmonary artery wedge pressure of 12 mmHg. The patient has been receiving intravenous epoprostenol, home oxygen therapy, sildenafil, bosentan, cardiotoxic drugs, anticoagulants, and diuretics. The current condition of the patient at 18 years old is WHO functional class III. Currently, the patient and her family do not wish to undergo lung transplantation.

The patient’s history includes Graves’ disease, which occurred at 13 years old. She initially received thiamazole; however, she stopped that treatment and began potassium iodide because of agranulocytosis. Thyroidectomy was not approved because of severe PH.

Decreased expression of NOTCH3 and ER-Resident chaperones in mutant cell lines

According to a previous report (Takahashi et al. 2010), we established stable HEK293 cell lines in which the expression of NOTCH3 was inducible using the tetracycline-on (Tet-on) regulatory system (T-REx System; Invitrogen). Several cell lines were established, and three cell lines for each construct were selected for NOTCH3 expression experiments. The expression of the mutant versions of NOTCH3 was lower than that of wild-type NOTCH3 (Fig. 3). Additionally, the expression levels of three endoplasmic reticulum (ER)-resident chaperones, GRP78/BiP, Calnexin, and ERp72, were higher in cells overexpressing wild-type NOTCH3 than in cells overexpressing the NOTCH3 mutants, particularly for the T900P-NOTCH3 mutant (Figs. 3A and S2). In Figure S3, the mutant NOTCH3 protein disappeared more quickly than wild-type NOTCH3 protein. Based on the result, the lower expression levels of mutant NOTCH3 in Figure 3A were caused by the high clearance speed.

NOTCH3 mutants fail to fully bind to GRP78/BiP

On the basis of the findings illustrated in Figure 3A, we investigated whether mutant NOTCH3 interacts with ER chaperones. As shown in Figure 3B, GRP78/BiP coimmunoprecipitated with wild-type NOTCH3, indicating

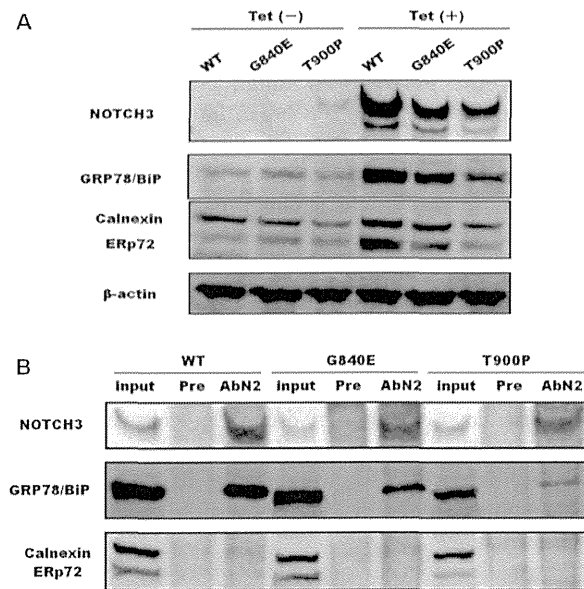


Figure 3. Expression of NOTCH3 and the endoplasmic reticulum (ER) chaperones. (A) Stable cells were incubated with or without 2 $\mu\text{g}/\text{mL}$ tetracycline (Tet) for 24 h and these cell lysates (12 μg) were subjected to SDS-gel electrophoresis. We assessed more than three stable cell lines for each of the wild-type and mutant NOTCH3 proteins. The experiment was performed three times. (B) Interaction between ER chaperones and NOTCH3. Cell lysates (200 μg) from stable cell lines were subjected to immunoprecipitation using an anti-NOTCH3 antibody (AbN2) or preimmune rabbit IgG (Pre). Immunoprecipitated complexes were subjected to SDS-PAGE and western blotting. The experiments were performed in triplicate for each stable cell line (WT-17, G840E-36, and T900P-33).

that wild-type NOTCH3 interacted with this ER chaperone. The amount of GRP78/BiP that coprecipitated with the NOTCH3 mutants was markedly lower than the amount that coprecipitated with wild-type NOTCH3. Calnexin and ERp72 were not detected in any of the wild-type or mutant NOTCH3-immunoprecipitated samples.

Changes in NOTCH3 levels and GRP78/BiP localization

We examined the quantity and localization of wild-type or mutant NOTCH3 via immunostaining using the ER marker GRP78/BiP. While many wild-type NOTCH3 aggregates were detected in the perinuclear region of the cytoplasm, very few mutant NOTCH3 perinuclear aggregates were detected, particularly in cells transfected with T900P-NOTCH3 (Fig. 4A). Aggregates were colocalized with GRP78/BiP in cells expressing wild-type NOTCH3. However, in cells expressing G840E-NOTCH3, GRP78/

BiP was partly localized in the nucleus and did not fully colocalize with NOTCH3 aggregates. This was particularly evident in cells expressing T900P-NOTCH3. When present in the nucleus, GRP78/BiP was colocalized with nuclear bodies (Fig. 4A).

Clearance of NOTCH3 aggregates

We next examined the degradation of wild-type and mutant NOTCH3 aggregates after 2 days using Tet-on cells. Figure 4B shows that wild-type NOTCH3 and G840E-NOTCH3 aggregates degraded slowly, whereas T900P-NOTCH3 aggregates disappeared rapidly. As was the case for stable cells immediately after Tet-on, GRP78/BiP was located in the nucleus in cells expressing mutant NOTCH3, most notably in cells expressing T900P-NOTCH3. These findings were confirmed by western blotting of cells expressing NOTCH3 (Fig. S3).

Promotion of cell proliferation and viability by mutant NOTCH3 expression

Cell proliferation was assessed by cell counting at 1 day, 3 days, and 5 days after Tet-on. The expression of wild-type NOTCH3 in the Tet-on cells caused a decrease in cell number compared to the untreated cells; however, the expression of mutant NOTCH3 had little impact on cell growth (Fig. 5A). We evaluated the ratio of the number of Tet-on cells to that of untreated cells on day 5 (Fig. 5A). The ratio of G840E-36 (0.78 ± 0.05) and T900P (0.70 ± 0.10) were significantly higher than that of WT-17 (0.50 ± 0.04 , $P = 0.004$ and 0.021 , respectively). These findings were confirmed via a cell proliferation assay using the WST-1 reagent (Fig. 5B and 5C). While the cells expressing wild-type NOTCH3 showed viability that was equivalent to that of untreated cells, the cells expressing mutant NOTCH3 exhibited a significantly higher level of viability. These cells reached confluence and did not show any detectable apoptosis or morphological abnormalities.

The NOTCH3 mutant induces the downregulation of NOTCH3-HES5 signaling activity

We investigated the transcriptional activity mediated by wild-type or mutant NOTCH3 with or without Jagged-1 to determine whether mutant NOTCH3 could increase or decrease NOTCH3-responsive target gene activity. To this end, we used a pHes5-luc reporter, where the luciferase Hes5 promoter drives expression to assess NOTCH3 activity. The luciferase assay showed that wild-type NOTCH3 exhibited significantly higher luciferase activity

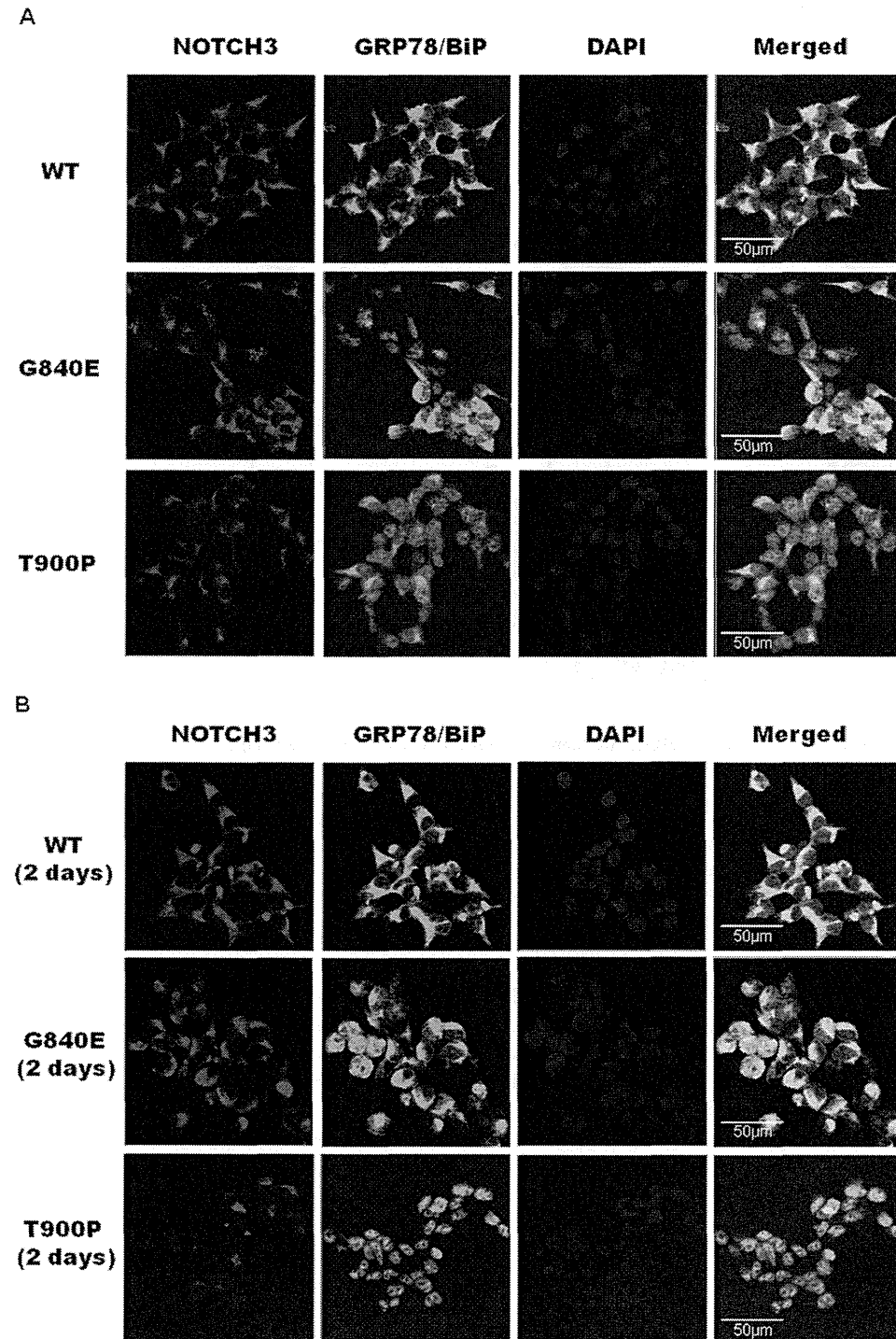


Figure 4. Changes in the quantity of NOTCH3 aggregates and the localization of GRP78/BiP. (A) Nine stable cell lines (WT-17, WT-21, WT-38, G840E-5, G840E-21, G840E-36, T900P-14, T900P-28, and T900P-33) were treated with 2 μ g/mL tetracycline for 24 h and double-stained with an anti-Notch3 antibody (AbN2) and a GRP78/BiP antibody. NOTCH3 (red) was detected by an Alexa Fluor 568-labeled secondary antibody and GRP78/BiP (green) was detected by an Alexa Fluor 488-labeled secondary antibody. (B) Stable cells were treated with tetracycline for 24 h and then incubated without tetracycline for 2 days. Cells were double-stained as described above.

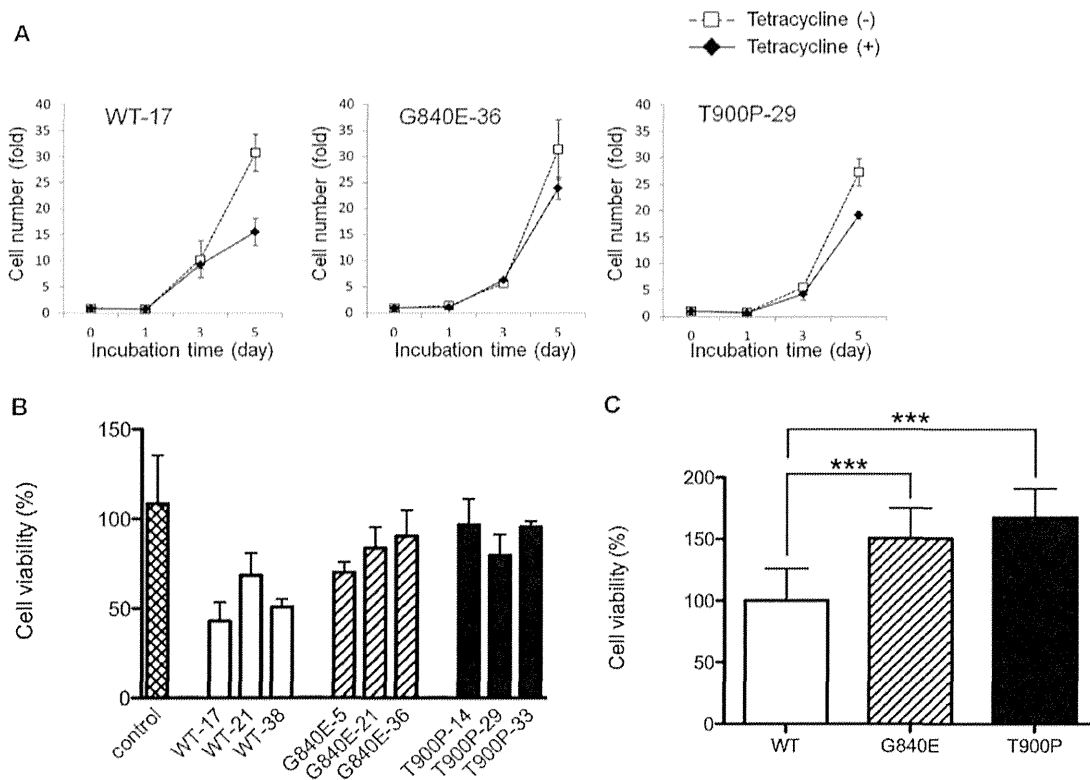


Figure 5. Cell proliferation and viability of *NOTCH3*. (A) Stable cells were incubated with (closed argyles) or without (open squares) tetracycline and harvested on days 0, 1, 3, and 5 for each of the nine stable cell lines (WT-17, WT-21, WT-38, G840E-5, G840E-21, G840E-36, T900P-14, T900P-29, and T900P-33). Each data point represents the mean number of cells with the standard deviation from four independent experiments. (B) Stable cells were incubated with or without tetracycline for 3 days. Cell viability was determined using the WST-1 reagent. The control indicates T-REX 293 cells that were not transfected. Values represent the means with the standard deviation from three independent experiments and are shown as the percentage of the total number of cells without tetracycline treatment. (C) The cell viability demonstrated in (B) was converted to a percentage of the mean value relative to that of stable cells expressing wild-type *NOTCH3*. Each data point represents the mean and standard deviation from nine cell lines. *** $P < 0.001$.

with Jagged-1 stimulation than without Jagged-1 stimulation. After stimulation with Jagged-1, however, G840E-*NOTCH3* and T900P-*NOTCH3* did not induce higher activity than mutant *NOTCH3* without Jagged-1 stimulation (Fig. 6). These findings indicated that *NOTCH3* mutants induced an impairment in *NOTCH3*-HES5 signaling.

Discussion

This is the first study to report the identification of two missense mutations in *NOTCH3* in IPAH patients. Both of the mutations identified in this study result in amino acid substitutions in the highly conserved and functionally essential EGF-like domain, and both mutations were absent in 170 Japanese and 300 Caucasian healthy controls, the 1000 Genomes Database, and the EVS Database.

NOTCH genes encode a group of 300-kD single-pass transmembrane receptors (*NOTCH1–4*). The large extracellular domain contains tandem EGF-like repeats and cysteine-rich Notch/LIN-12 repeats, and Ankyrin repeats and a PEST sequence have been found within the intracellular domain (ICD) (Artavanis-Tsakonas et al. 1999). The *NOTCH* signaling pathway is highly evolutionarily conserved and is critical for cell fate determination during embryonic development, including many aspects of vascular development (Wang et al. 2008). Upon interacting with its ligands (Jagged-1, Jagged-2, and Delta family) expressed on neighboring cells, *NOTCH* undergoes proteolytic cleavage, which frees the ICD from the plasma membrane (Xia et al. 2012). This change induces translocation of the ICD into the nucleus. The ICD then forms a complex with the transcriptional repressor CBF1/RBP-jk, which induces the transcription of downstream target genes, including

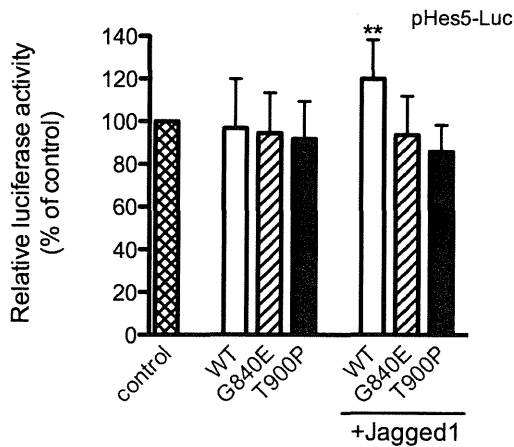


Figure 6. Luciferase activity induced by *NOTCH3*. T-REx 293 cells were transfected with pHes5-Luc and any one of wild-type *NOTCH3*, mutant *NOTCH3*, or the empty pcDNA4/TO vector. Some of the cells were cultured with preclustered Jagged-1 Fc (100 ng/mL) for 4 h. Values represent the mean with standard deviation of four independent experiments. The means were compared with wild-type (WT without stimulation with Jagged-1) using one-way ANOVA followed by Dunnett's test. ** $P < 0.01$.

HES1/5/7 and the *HEY* family genes (Iso et al. 2003; Weber 2008).

NOTCH3 is predominantly expressed in arterial vascular SMCs, where it regulates SMC differentiation (Zhu et al. 2011; Xia et al. 2012). The main *NOTCH3* ligand is Jagged-1, which is also expressed in arterial endothelial cells (ECs) (Xia et al. 2012). Taking these reports into consideration, we decided to perform functional analysis of mutant *NOTCH3* through the use of Jagged-1 Fc.

NOTCH3 mutations are known to be associated with cerebral autosomal dominant arteriopathy with subcortical infarcts and leukoencephalopathy (CADASIL) (Joutel et al. 1996). More than 150 *NOTCH3* mutations have been reported in CADASIL patients; mutation hot spots are located in exons 3 and 4 (Chabriat et al. 2009). Both of the *NOTCH3* mutations that we identified in IPAH patients were missense mutations located in exons 16 and 17. To date, no mutations in these two exons have been reported in CADASIL patients, and there have been no reports of a PAH complication in CADASIL.

In this study, we revealed that compared to the wild-type protein, mutant *NOTCH3* formed aggregates poorly and decreased the amount of GRP78/BiP, Calnexin, and ERP72. Our immunoprecipitation studies suggested that GRP78/BiP cannot interact with mutant *NOTCH3*. In addition, we found that T900P-*NOTCH3* was degraded more rapidly than wild-type *NOTCH3*. These findings are not consistent with a previous report that

investigated CADASIL mutations using similar methods (Takahashi et al. 2010); however, these differences may be attributable to the difference in the location of the mutations.

In an immunocytochemistry study, we indicated that GRP78/BiP and wild-type *NOTCH3* were colocalized in the ER, and that GRP78/BiP was localized in the nuclei of cells expressing mutant *NOTCH3*. GRP78, a member of the HSP70 gene family, has been traditionally regarded as a major ER chaperone that facilitates protein folding and assembly, protein quality control, Ca^{2+} binding, and the regulation of ER stress signaling (Ni et al. 2011). It is also known that GRP78 can be observed in the nucleus when it is ectopically overexpressed or induced by ER stress (Reddy et al. 2003; Huang et al. 2009). On the basis of this information, we hypothesize that the mutant *NOTCH3* protein induces a high level of stress on the ER and induces GRP78/BiP nuclear translocation. Because the mutant *NOTCH3* protein is located in the ER, it may not be able to interact with GRP78/BiP in the nucleus. Gene mutations can cause aberrant protein folding and the accumulation of the mutant protein in the ER (Takahashi et al. 2010). Because ER chaperones facilitate ER-associated protein degradation to clear aggregated, misfolded, or unassembled proteins (Ni and Lee 2007), T900P-*NOTCH3* proteins may be degraded more rapidly than wild-type *NOTCH3*.

The cells expressing mutant *NOTCH3* showed higher levels of viability and proliferation than the cells expressing wild-type *NOTCH3*, and did not exhibit apoptosis or morphological abnormalities. These findings suggest that when the normal *NOTCH3* protein is absent, increases in cell proliferation rates occur. This result is contrary to the work of Li et al. and taken together the role of *NOTCH3* may be more complex than first described. Thus more work is required to resolve this discrepancy.

In the luciferase assay, we showed that the *NOTCH3* mutations we identified caused an impairment in *NOTCH3*-*HES5* signaling activity. It remains unclear whether the *NOTCH3* mutations identified in this study affect *NOTCH* signaling activity. One study revealed that a part of the mutations identified in CADASIL patients caused a gain in function in the *NOTCH* signaling pathway (Joutel et al. 2004). Another report indicated that *NOTCH3* mutations in or near the ligand-binding site (EGF-like repeats 10-11, corresponding to a part of exon 7-9) impaired ligand binding sufficiently to affect signaling activity (Peters et al. 2004). Furthermore, another two studies suggested that most of the mutations located outside of the ligand-binding site did not impair the signal transduction activity of *NOTCH3* (Low et al. 2006; Monet-Leprêtre et al. 2009). The difference in function

between exon 16–17, in which the mutations we identified were located, and other exons corresponding to EGF-like repeats remain unexplained. Further investigations are necessary.

It appears that epoprostenol may not be sufficiently effective in the two PAH patients with *NOTCH3* mutations. Although the reason remains unclear, epoprostenol might not influence to *NOTCH* signaling. In addition, their age at diagnosis was very young comparatively. It was difficult to identify other additional phenotypic features in the two subjects. The youngest elder brother of proband B has the same *NOTCH3* mutation, but has not exhibited any clinical signs of PAH to date. The *NOTCH3* mutation may have very low penetrance in familial PAH, as well as *BMP2* mutation in familial PAH. In CADASIL patients, the penetrance of *NOTCH3* mutation is complete by the end of fourth decade (Ayata 2010). Although we cannot clarify whether the youngest elder brother of proband B will develop PAH in the future, it will be necessary to check his health condition periodically.

We identified several limitations of our study. For the *NOTCH3* mutations we identified, a detailed investigation in a larger number of subjects is needed, and a search for mutations of other *NOTCH3* pathway genes may also be beneficial. Moreover, although we demonstrated that the mutant *NOTCH3* reduced the amount of GRP78/BiP, Dromparis et al. (2013) reported that the expression of GRP78 was increased in chronic normobaric hypoxia-pulmonary hypertension mice. These differences may be a result of the different types of mutations, cells, or species used in the various studies. We acknowledge that the HEK293 cells we used are not the ideal cell lines for functional studies of PAH; thus, it is difficult to prove definitively that *NOTCH3* causes PAH based on our findings. However, in the study conducted by Dromparis et al. (2013), it seems that GRP78 was translocated to the nucleus in the pulmonary artery SMCs of hypoxia mice more than normoxia mice. Because this finding is consistent with our immunostaining results, the study supports our hypothesis that mutant *NOTCH3* induces a high degree of ER stress. Therefore, additional investigations are necessary to further analyze the function of *NOTCH3* in the pathogenesis of PAH. These studies might include cell proliferation and viability analyses using both ECs and SMCs from human pulmonary arteries and animal models with the *NOTCH3* mutation.

Acknowledgments

We are grateful to the patients and their family members. We thank Atsushi Watanabe and Ryoichiro Kageyama for providing the plasmids. We thank Ryohei Tsutsumi

for his excellent technical assistance. We also thank Rumi-ko Matsuoka for her supervision.

Conflict of Interest

None declared.

References

- Adzhubei, I. A., S. Schmidt, L. Peshkin, V. E. Ramensky, A. Gerasimova, P. Bork, et al. 2010. A method and server for predicting damaging missense mutations. *Nat. Methods* 7:248–249.
- Artavanis-Tsakonas, S., M. D. Rand, and R. J. Lake. 1999. Notch signaling: cell fate control and signal integration in development. *Science* 284:770–776.
- Austin, E. D., L. Ma, C. LeDuc, E. Berman Rosenzweig, A. Borczuk, J. A. Phillips, III, et al. 2012. Whole exome sequencing to identify a novel gene (caveolin-1) associated with human pulmonary arterial hypertension. *Circ. Cardiovasc. Genet.* 5:336–343.
- Ayata, C. 2010. CADASIL: experimental insights from animal models. *Stroke* 41(10 Suppl.):S129–S134.
- Chabriat, H., A. Joutel, M. Dichgans, E. Tournier-Lasserre, and M. G. Bousser. 2009. Cadasil. *Lancet Neurol.* 8:643–653.
- Chida, A., M. Shintani, T. Nakayama, Y. Furutani, E. Hayama, K. Inai, et al. 2012. Missense mutations of the *BMPRIIB* (*ALK6*) gene in childhood idiopathic pulmonary arterial hypertension. *Circ. J.* 76:1501–1508.
- Deng, Z., J. H. Morse, S. L. Slager, N. Cuervo, K. J. Moore, G. Venetos, et al. 2000. Familial primary pulmonary hypertension (gene *PPH1*) is caused by mutations in the bone morphogenetic protein receptor-II gene. *Am. J. Hum. Genet.* 67:737–744.
- Dromparis, P., R. Paulin, T. H. Stenson, A. Haromy, G. Sutendra, and E. D. Michelakis. 2013. Attenuating endoplasmic reticulum stress as a novel therapeutic strategy in pulmonary hypertension. *Circulation* 127:115–125.
- Gainé, S. P., and L. J. Rubin. 1998. Primary pulmonary hypertension. *Lancet* 352:719–725.
- Galiè, N., M. M. Hoeper, M. Humbert, A. Torbicki, J. L. Vachiery, J. A. Barbera, et al. 2009. Guidelines for the diagnosis and treatment of pulmonary hypertension: the Task Force for the Diagnosis and Treatment of Pulmonary Hypertension of the European Society of Cardiology (ESC) and the European Respiratory Society (ERS), endorsed by the International Society of Heart and Lung Transplantation (ISHLT). ESC Committee for Practice Guidelines (CPG). *Eur. Heart J.* 30:2493–2537.
- Harrison, R. E., J. A. Flanagan, M. Sankelo, S. A. Abdalla, J. Rowell, R. D. Machado, et al. 2003. Molecular and functional analysis identifies *ALK-1* as the predominant cause of pulmonary hypertension related to hereditary haemorrhagic telangiectasia. *J. Med. Genet.* 40:865–871.

- Harrison, R. E., R. Berger, S. G. Haworth, R. Tulloh, C. J. Mache, N. W. Morrell, *et al.* 2005. Transforming growth factor-beta, receptor mutations and pulmonary arterial hypertension in childhood. *Circulation* 111:435–441.
- Huang, S. P., J. C. Chen, C. C. Wu, C. T. Chen, N. Y. Tang, Y. T. Ho, *et al.* 2009. Capsaicin-induced apoptosis in human hepatoma HepG2 cells. *Anticancer Res.* 29: 165–174.
- Iso, T., Y. Hamamori, and L. Kedes. 2003. Notch signaling in vascular development. *Arterioscler. Thromb. Vasc. Biol.* 23:543–553.
- Joutel, A., C. Corpechot, A. Ducros, K. Vahedi, H. Chabriat, P. Mouton, *et al.* 1996. Notch3 mutations in CADASIL, a hereditary adult-onset condition causing stroke and dementia. *Nature* 383:707–710.
- Joutel, A., M. Monet, V. Domenga, F. Riant, and E. Tournier-Lasserre. 2004. Pathogenic mutations associated with cerebral autosomal dominant arteriopathy with subcortical infarcts and leukoencephalopathy differently affect Jagged1 binding and Notch3 activity via the RBP/JK signaling pathway. *Am. J. Hum. Genet.* 74:338–347.
- Kumar, P., S. Henikoff, and P. C. Ng. 2009. Predicting the effects of coding non-synonymous variants on protein function using the SIFT algorithm. *Nat. Protoc.* 4: 1073–1081.
- Lane, K. B., R. D. Machado, M. W. Pauciulo, J. R. Thomson, J. A. Phillips, III, J. E. Loyd, *et al.* 2000. Heterozygous germline mutations in *BMPR2*, encoding a TGF-beta receptor, cause familial primary pulmonary hypertension: the International PPH Consortium. *Nat. Genet.* 26:81–84.
- Li, X., X. Zhang, R. Leathers, A. Makino, C. Huang, P. Parsa, *et al.* 2009. Notch3 signaling promotes the development of pulmonary arterial hypertension. *Nat. Med.* 15:1289–1297.
- Low, W. C., Y. Santa, K. Takahashi, T. Tabira, and R. N. Kalaria. 2006. CADASIL-causing mutations do not alter Notch3 receptor processing and activation. *NeuroReport* 17:945–949.
- Machado, R. D., O. Eickelberg, C. G. Elliott, M. W. Geraci, M. Hanaoka, J. E. Loyd, *et al.* 2009. Genetics and genomics of pulmonary arterial hypertension. *J. Am. Coll. Cardiol.* 54(1 Suppl.):S32–S42.
- Monet-Leprêtre, M., B. Bardot, B. Lemaire, V. Domenga, O. Godin, M. Dichgans, *et al.* 2009. Distinct phenotypic and functional features of CADASIL mutations in the Notch3 ligand binding domain. *Brain* 132:1601–1612.
- Nasim, M. T., T. Ogo, M. Ahmed, R. Randall, H. M. Chowdhury, K. M. Snape, *et al.* 2012. Molecular genetic characterization of SMAD signaling molecules in pulmonary arterial hypertension. *Hum. Mutat.* 32:1385–1389.
- Ni, M., and A. S. Lee. 2007. ER chaperones in mammalian development and human diseases. *FEBS Lett.* 581:3641–3651.
- Ni, M., Y. Zhang, and A. S. Lee. 2011. Beyond the endoplasmic reticulum: atypical GRP78 in cell viability, signalling and therapeutic targeting. *Biochem. J.* 434:181–188.
- Peters, N., C. Opherck, S. Zacherle, A. Capell, P. Gempel, and M. Dichgans. 2004. CADASIL-associated Notch3 mutations have differential effects both on ligand binding and ligand-induced Notch3 receptor signaling through RBP-Jk. *Exp. Cell Res.* 299:454–464.
- Reddy, R. K., C. Mao, P. Baumeister, R. C. Austin, R. J. Kaufman, and A. S. Lee. 2003. Endoplasmic reticulum chaperone protein GRP78 protects cells from apoptosis induced by topoisomerase inhibitors: role of ATP binding site in suppression of caspase-7 activation. *J. Biol. Chem.* 278:20915–20924.
- Shintani, M., H. Yagi, T. Nakayama, T. Saji, and R. Matsuoka. 2009. A new nonsense mutation of *SMAD8* associated with pulmonary arterial hypertension. *J. Med. Genet.* 46:331–337.
- Simonneau, G., I. M. Robbins, M. Beghetti, R. N. Channick, M. Delcroix, C. P. Denton, *et al.* 2009. Updated clinical classification of pulmonary hypertension. *J. Am. Coll. Cardiol.* 54(1 Suppl.):S43.
- Takahashi, K., K. Adachi, K. Yoshizaki, S. Kunimoto, R. N. Kalaria, and A. Watanabe. 2010. Mutations in *NOTCH3* cause the formation and retention of aggregates in the endoplasmic reticulum, leading to impaired cell proliferation. *Hum. Mol. Genet.* 19:79–89.
- Trembath, R. C., J. R. Thomson, R. D. Machado, N. V. Morgan, C. Atkinson, I. Winship, *et al.* 2001. Clinical and molecular genetic features of pulmonary hypertension in patients with hereditary hemorrhagic telangiectasia. *N. Engl. J. Med.* 345:325–334.
- Wang, T., M. Baron, and D. Trump. 2008. An overview of Notch3 function in vascular smooth muscle cells. *Prog. Biophys. Mol. Biol.* 96:499–509.
- Weber, D. S. 2008. A novel mechanism of vascular smooth muscle cell regulation by Notch: platelet-derived growth factor receptor-beta expression? *Circ. Res.* 102:1448–1450.
- Xia, Y., A. Bhattacharyya, E. E. Roszell, M. Sandig, and K. Mequanint. 2012. The role of endothelial cell-bound Jagged1 in Notch3-induced human coronary artery smooth muscle cell differentiation. *Biomaterials* 33:2462–2472.
- Zhu, J. H., C. L. Chen, S. Flavahan, J. Harr, B. Su, and N. A. Flavahan. 2011. Cyclic stretch stimulates vascular smooth muscle cell alignment by redox-dependent activation of Notch3. *Am. J. Physiol. Heart Circ. Physiol.* 300:H1770–H1780.

Supporting Information

Additional Supporting Information may be found in the online version of this article:

Data S1. Supplementary Methods

Table S1. Primer pairs used to amplify the *NOTCH3*, *HES1*, and *HES5* coding sequences.

Figure S1. Sequence analysis of the *NOTCH3* mutation in the family of proband B.

Figure S2. Mean ER chaperone/ β -actin ratios from densitometry analysis of data presented in Figure 3. The levels of all three chaperones were significantly decreased in cells expressing T900P-*NOTCH3* compared with those expressing wild-type *NOTCH3* (WT). * $P < 0.05$.

Figure S3. Western blotting of *NOTCH3* degradation.

Stable cells were treated with (Tet+) or without (Tet-) tetracycline (2 $\mu\text{g}/\text{mL}$) for 24 h and then incubated in medium without tetracycline. Cells were harvested on days 0, 1, and 2 and were subjected to SDS-PAGE and western blot analysis. The data are representative of experiments performed for three stable cell lines (WT-17, G840E-36, and T900P-33). Experiments were performed twice for each stable cell line.



Primary immunodeficiency diseases: an update on the classification from the International Union of Immunological Societies Expert Committee for Primary Immunodeficiency

Waleed Al-Herz^{1,2}, Aziz Bousfiha³, Jean-Laurent Casanova^{4,5}, Talal Chatila⁶, Mary Ellen Conley⁴, Charlotte Cunningham-Rundles⁷, Amos Etzioni⁸, Jose Luis Franco⁹, H. Bobby Gaspar^{10*}, Steven M. Holland¹¹, Christoph Klein¹², Shigeaki Nonoyama¹³, Hans D. Ochs¹⁴, Erik Oksenhendler^{15,16}, Capucine Picard^{5,17}, Jennifer M. Puck¹⁸, Kate Sullivan¹⁹ and Mimi L. K. Tang^{20,21,22}

¹ Department of Pediatrics, Kuwait University, Kuwait City, Kuwait

² Allergy and Clinical Immunology Unit, Department of Pediatrics, Al-Sabah Hospital, Kuwait City, Kuwait

³ Clinical Immunology Unit, Casablanca Children's Hospital, Ibn Rochd Medical School, King Hassan II University, Casablanca, Morocco

⁴ St. Giles Laboratory of Human Genetics of Infectious Diseases, Rockefeller Branch, The Rockefeller University, New York, NY, USA

⁵ Laboratory of Human Genetics of Infectious Diseases, Necker Branch, INSERM UMR1163, Imagine Institut, Necker Medical School, University Paris Descartes, Paris, France

⁶ Division of Immunology, Children's Hospital Boston, Boston, MA, USA

⁷ Department of Medicine and Pediatrics, Mount Sinai School of Medicine, New York, NY, USA

⁸ Meyer Children's Hospital-Technion, Haifa, Israel

⁹ Group of Primary Immunodeficiencies, University of Antioquia, Medellin, Colombia

¹⁰ UCL Institute of Child Health, London, UK

¹¹ Laboratory of Clinical Infectious Diseases, National Institute of Allergy and Infectious Diseases, Bethesda, MD, USA

¹² Dr. von Hauner Children's Hospital, Ludwig-Maximilians-University Munich, Munich, Germany

¹³ Department of Pediatrics, National Defense Medical College, Saitama, Japan

¹⁴ Department of Pediatrics, Seattle Children's Research Institute, University of Washington, Seattle, WA, USA

¹⁵ Department of Clinical Immunology, Hôpital Saint-Louis, Assistance Publique-Hôpitaux de Paris, Paris, France

¹⁶ Sorbonne Paris Cité, Université Paris Diderot, Paris, France

¹⁷ Centre d'Étude des Déficiences Immunitaires (CEDi), Hôpital Necker-Enfants Malades, AP-HP, Paris, France

¹⁸ Department of Pediatrics, UCSF Benioff Children's Hospital, University of California San Francisco, San Francisco, CA, USA

¹⁹ Department of Pediatrics, Division of Allergy Immunology, The Children's Hospital of Philadelphia, Philadelphia, PA, USA

²⁰ Murdoch Children's Research Institute, Melbourne, VIC, Australia

²¹ Department of Paediatrics, University of Melbourne, Melbourne, VIC, Australia

²² Department of Allergy and Immunology, Royal Children's Hospital, Melbourne, VIC, Australia

Edited by:

Jordan Orange, Baylor College of Medicine, USA

Reviewed by:

Jordan Orange, Baylor College of Medicine, USA

Francisco A. Bonilla, Boston Children's Hospital, USA

Thomas Arthur Fleisher, National Institutes of Health, USA

Fischer Alain, INSERM, France

*Correspondence:

H. Bobby Gaspar, Molecular Immunology Unit, UCL Institute of Child Health, 30 Guilford Street, London WC1N 1EH, UK
e-mail: h.gaspar@ucl.ac.uk

We report the updated classification of primary immunodeficiencies (PIDs) compiled by the Expert Committee of the International Union of Immunological Societies. In comparison to the previous version, more than 30 new gene defects are reported in this updated version. In addition, we have added a table of acquired defects that are phenocopies of PIDs. For each disorder, the key clinical and laboratory features are provided. This classification is the most up-to-date catalog of all known PIDs and acts as a current reference of the knowledge of these conditions and is an important aid for the molecular diagnosis of patients with these rare diseases.

Keywords: primary immunodeficiencies, IUIS, classification, genetic defects, genotype

BACKGROUND

The International Union of Immunological Societies (IUIS) Expert Committee on Primary Immunodeficiency met in New York on 19th–21st April 2013 to update the classification of human primary immunodeficiencies (PIDs). This report represents the most current and complete catalog of known PIDs. It serves as a reference for these conditions and provides a framework to help in the diagnostic approach to patients suspected to have PID.

As in previous reports, we have classified the conditions into major groups of PIDs and these are now represented in nine different tables. In each table, we list the condition, its genetic defect if known, and the major immunological and in some conditions the non-immunological abnormalities associated with the disease. The classification this year differs slightly from the previous edition in that **Table 1** lists combined immunodeficiencies without non-immunologic phenotypes, whereas **Table 2** refers to combined

Table 1 | Combined immunodeficiencies.

Disease	Genetic defect/ presumed pathogenesis	Inheritance	Circulating T cells	Circulating B cells	Serum Ig	Associated features	OMIM number
1. T ⁺ B ⁺ severe combined immunodeficiency (SCID)							
(a) γ c deficiency	Mutation of <i>IL2RG</i> Defect in γ chain of receptors for IL-2, -4, -7, -9, -15, -21	XL	Markedly decreased	Normal or increased	Decreased	Markedly decreased NK cells	300400
(b) JAK3 deficiency	Mutation of <i>JAK3</i> Defect in Janus-activating kinase 3	AR	Markedly decreased	Normal or increased	Decreased	Markedly decreased NK cells	600173
(c) IL7R α deficiency	Mutation of <i>IL7RA</i> Defect in IL-7 receptor α chain	AR	Markedly decreased	Normal or increased	Decreased	Normal NK cells	146661
(d) CD45 deficiency*	Mutation of <i>PTPRC</i> Defect in CD45	AR	Markedly decreased	Normal	Decreased	Normal γ/δ T cells	151460
(e) CD3 δ deficiency	Mutation of <i>CD3D</i> Defect in CD3 δ chain of T cell antigen receptor complex	AR	Markedly decreased	Normal	Decreased	Normal NK cells No γ/δ T cells	186790
(f) CD3 ϵ deficiency*	Mutation of <i>CD3E</i> Defect in CD3 ϵ chain of T cell antigen receptor complex	AR	Markedly decreased	Normal	Decreased	Normal NK cells No γ/δ T cells	186830
(g) CD3 ζ deficiency*	Mutation of <i>CD3Z</i> Defect in CD3 ζ chain of T cell antigen receptor complex	AR	Markedly decreased	Normal	Decreased	Normal NK cells No γ/δ T cells	186740
(h) Coronin-1A deficiency*	Mutation of <i>CORO1A</i> defective thymic egress of T cells and defective T cell locomotion	AR	Markedly decreased	Normal	Decreased	Detectable thymus EBV associated B cell lymphoproliferation	605000
2. T ⁻ B ⁻ SCID							
(i) DNA recombination defects							
(a) RAG 1 deficiency	Mutation of <i>RAG1</i> Defective VDJ recombination; defect of recombinase activating gene (RAG) 1	AR	Markedly decreased	Markedly decreased	Decreased		601457
(a) RAG 2 deficiency	Mutation of <i>RAG2</i> Defective VDJ recombination; defect of recombinase activating gene (RAG) 2	AR	Markedly decreased	Markedly decreased	Decreased		601457
(b) DCLRE1C (artemis) deficiency	Mutation of <i>ARTEMIS</i> Defective VDJ recombination; defect in artemis DNA recombinase repair protein	AR	Markedly decreased	Markedly decreased	Decreased	Radiation sensitivity	602450
(c) DNA PKcs deficiency*	Mutation of <i>PRKDC</i> - Defective VDJ recombination; defect in DNA PKcs Recombinase repair protein	AR	Markedly decreased	Markedly decreased	Decreased	Radiation sensitivity, microcephaly, and developmental defects	600899
(ii) Reticular dysgenesis, AK2 deficiency	Mutation of <i>AK2</i> Defective maturation of lymphoid and myeloid cells (stem cell defect) Defect in mitochondrial adenylate kinase 2	AR	Markedly decreased	Decreased or normal	Decreased	Granulocytopenia and deafness	103020

(Continued)